

1 **Title**

2 Evaluating the Potential of Full-waveform Lidar for Mapping Pan-Tropical Tree Species Richness

3

4 **Short title**

5 Lidar and Pan-Tropical Tree Species Richness

6

7 **Abstract**

8 **Aim:**

9 Mapping tree species richness across the tropics is of great interest for effective conservation and
10 biodiversity management. In this study, we evaluated the potential of full-waveform lidar data for
11 mapping tree species richness across the tropics by relating measurements of vertical canopy structure,
12 as a proxy for the occupation of vertical niche space, to tree species richness.

13 **Location:**

14 Tropics

15 **Time period:**

16 Present

17 **Major taxa studied:**

18 Trees

19 **Methods:**

20 First, we evaluated the characteristics of vertical canopy structure across 15 moist forest study sites
21 using (simulated) large-footprint full-waveform lidar data (22 m diameter) and related findings to in-situ
22 tree species information. Then, we developed structure-richness models at the local (within 25-50 ha
23 plots), regional (biogeographic regions), and pan-tropical scale at three spatial resolutions (1.0, 0.25 and
24 0.0625 ha) using Poisson regression.

25 **Results:**

26 The results showed a weak structure-richness relationship at the local scale. At the regional scale (within
27 a biogeographical region) a stronger relationship between canopy structure and tree species richness
28 across different tropical forest types was found, for example across Central Africa and in South America
29 (R^2 ranging from 0.44-0.56, RMSD ranging between 23-61%). Using a pan-tropical relationship, across
30 four continents, 39% of the variation in tree species richness could be explained with canopy structure
31 alone ($R^2 = 0.39$ and RMSE = 43%, 0.25 ha resolution).

32 **Main Conclusions:**

33 Our results may serve as a basis for the future development of a set of structure-richness models to map
34 tropical forest tree species richness at high resolution using vertical canopy structure information from
35 the Global Ecosystem Dynamics Investigation (GEDI). The value of this effort would be enhanced by
36 access to a larger set of field reference data for all tropical regions. Future research could also support
37 the use of GEDI data in frameworks using environmental and spectral information for modelling tree
38 species richness across the tropics.

39 **Keywords**

40 Biodiversity, canopy structure, GEDI, lidar, plant area index, tropical forests

41 **1. Introduction**

42 Tropical forests are known for their high tree species diversity. Current estimates suggest in the order of
43 15,000 tree species in Amazonia alone, in contrast to 124 tree species in temperate forests in Europe,
44 and more than 40,000 different tree species across the tropical region (Slik *et al.*, 2015; Ter Steege *et al.*,
45 2015). High levels of tree species richness support the provision of essential ecosystem services (e.g.,
46 Liang *et al.*, 2016). Unfortunately, 35% of pre-agricultural global forest cover has been lost over the past
47 300 years, largely due to increasing human pressures on the environment. Eighty-two percent of the
48 remaining forest is estimated to have experienced some degree of human impact (Watson *et al.*, 2018).
49 The Convention of Biological Diversity (CBD) and Group on Earth Observations Biodiversity Observation
50 Network (GEO BON) have developed a list of important variables aiming to provide quantitative
51 information on biodiversity to reach the Aichi biodiversity targets 2020 (Pereira *et al.*, 2013; Skidmore *et*
52 *al.*, 2015). Among the identified needs is the mapping of taxonomic diversity at high spatial resolution
53 over large scales (Pereira *et al.*, 2010). Here we focus on tree species diversity. The collection of tree
54 species diversity data is traditionally done in the field, and such information has previously been used to
55 create predictive maps of tree species richness across the globe at low spatial resolution (Kier *et al.*,
56 2005; Mutke & Barthlott, 2005). More recently, passive remote sensing data, such as optical imagery
57 from different airborne and spaceborne platforms, has been used in combination with field reference
58 data to predict tree species diversity in different regions (Foody & Cutler, 2006; Carlson *et al.*, 2007;
59 Féret & Asner, 2014; Rocchini *et al.*, 2016; Schäfer *et al.*, 2016; Bongalov *et al.*, 2019). Even though such
60 methods have been progressively developing over the last decade, they are not yet operational for
61 mapping tree species richness across the tropics due to, among others, a lack of consistent remote
62 sensing and training data over such scales, insufficient model accuracy and/or low spatial resolution.

63 The scientific community has called for bolder science in conservation strategies to enable effective
64 management of the Earth's forests and allow for better conservation of our natural ecosystems (Watson
65 *et al.*, 2016). In this study we focus on the use of active remote sensing, specifically lidar, for mapping
66 taxonomic tree species richness in the tropics. While local tropical forest species richness is largely
67 independent of biomass in intact forests (Sullivan *et al.*, 2017), and forest structure in terms of height
68 diameter relationships differ varies regionally as does species richness (Feldpausch *et al.* 2012
69 Biogeosciences), it remains unclear if substantial amounts of variation in species diversity are
70 associated with features of forest structure. Here, we explore for the first time whether small-scale
71 vertical canopy structure variation is significantly associated with the spatial variation in tropical tree
72 species richness. On a global scale it has previously been shown that canopy height explains a limited
73 portion of the variation in tree species diversity, as such data provide information on the available niche
74 space (Gatti *et al.*, 2017). It has since been hypothesized that including information on the vertical
75 canopy structure, must explain more of the variation in tree species diversity than canopy height alone;
76 as such data provide information on the occupation of the vertical niche space. Marselis *et al.* (2019)
77 demonstrated that information on canopy height and vertical canopy structure, expressed as the Plant
78 Area Index (PAI) profile from full-waveform airborne lidar data, could be used to map tree species
79 diversity in Gabon, Africa. However, it is not clear whether this relationship is of similar nature and
80 strength across different regions, or even the entire tropics. If existent, than the use of such a structure-
81 diversity relationship(s) could become operational at a pan-tropical scale with the rapidly increasing
82 availability of spaceborne canopy structure information derived from the Global Ecosystem Dynamics
83 Investigation (GEDI), a full-waveform spaceborne lidar system (Dubayah *et al.*, 2020). GEDI is expected
84 to provide over 10 billion measurements of vertical canopy structure across the temperate and tropical
85 forests between 2019 and 2021.

86 Factors influencing tree species diversity on a global scale differ from those affecting spatial patterns at
87 regional or local scales. In general, tropical tree species diversity increases with increasing precipitation,
88 forest stature, soil fertility, time since catastrophic disturbance and rate of canopy turnover and
89 decreases with seasonality, latitude, and altitude (Givnish, 1999). At large-grain scales historical
90 biogeography processes are more important, whereas at the plot-scale environmental variables strongly
91 influence diversity (Keil & Chase, 2019).

92 Similar to species diversity, forest structure at the global scale is influenced by interacting historic,
93 environmental, and human related variables; precipitation in the wettest month being the most
94 important single predictor of plant height (Moles *et al.*, 2009). Forest structure measured in the field is
95 mainly comprised of four variables: canopy height, biomass, basal area and tree density (Palace *et al.*,
96 2015). However, active remote sensing techniques have revolutionized the study of canopy structure
97 (Newnham *et al.*, 2015). With lidar remote sensing, for example, it is now possible to obtain information
98 on canopy height, as well as the position and amount of plant material along the vertical axis of the
99 canopy (Tang *et al.*, 2012). Palace *et al.* (2015) stressed that high resolution lidar data possess vertical
100 structure information which is inherently linked to ecological processes.

101 We hypothesize that structure-diversity relationships will vary across different biogeographical and
102 phylogenetic regions (Corlett & Primack, 2011; Slik *et al.*, 2018) and that it may be more fruitful to
103 develop multiple relationships rather than one pan-tropical relationship for operationalizing tree species
104 diversity mapping with spaceborne active remote sensing data. Additionally, the strength of the
105 relationship between a variable and tree species diversity often changes with resolution (plot size) as
106 tree species diversity is not linearly related with area (species-area curve) (MacArthur & Wilson, 1967).
107 This complicates the development of predictive models at specific resolutions, and also limits the
108 extrapolation of estimates at one resolution to a larger area, which impedes the mapping of pan-tropical
109 tree species diversity at high spatial resolution.

110 In sum, we know that both species diversity and canopy structure vary greatly within and across
111 continents. Hence, our objective is to assess whether canopy structure information can explain tree
112 species richness at the local, regional and/or pan-tropical scale with the ultimate goal to evaluate the
113 efficacy of spaceborne full-waveform lidar for mapping tree species richness across the tropics. First, we
114 compare characteristics of the vertical canopy structure, measured with full-waveform lidar data, of
115 tropical forests across the world. Second, we evaluate the differences in species richness and species-
116 area curves across the different study sites using field measurements. Third, we evaluate the potential
117 for developing local (within 25-50 ha field plots), regional (within biogeographical regions) and pan-
118 tropical structure-richness relationships, relating canopy structure metrics from lidar to tree species
119 richness measurements from the field at three spatial resolutions (0.0625, 0.25 and 1.0 ha). Lastly, we
120 discuss the potential of full-waveform lidar data from GEDI for mapping tree species richness across the
121 tropics using structure-richness relationships.

122 **2. Materials and Methods**

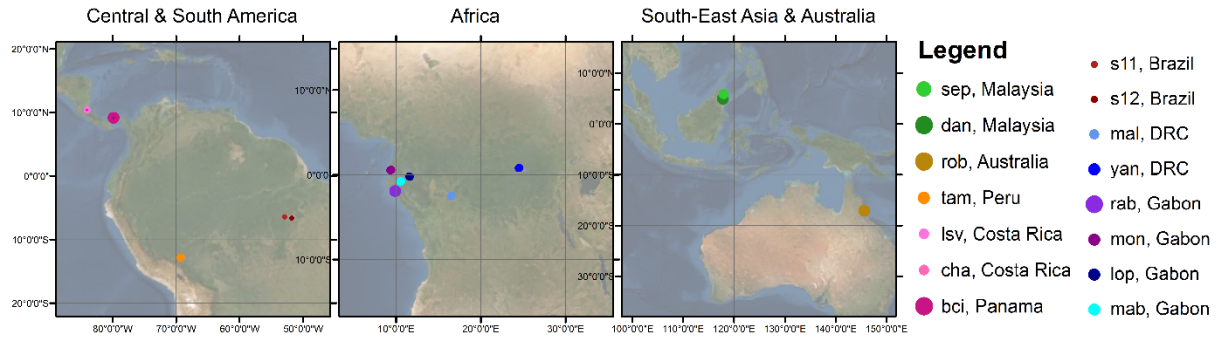
123 We address the relationship between canopy structure and tree species richness in *terra firme* lowland
124 moist forest in the tropical region between 23.5° N and S. We compiled a comprehensive field and lidar
125 dataset covering colonizing forest, old-growth tropical forest and forests under different degrees of
126 degradation and savanna. We included a wide variety of forest with differing degrees of disturbance
127 because most of the Earth's tropical forests have been degraded or otherwise affected by natural and
128 human influences (Lewis *et al.*, 2015). Hence, when developing a method that allows for estimating pan-
129 tropical tree species richness it is important to include data covering this range of possibilities.

130 Species diversity can be expressed with a variety of indicators. Generally, three levels of diversity are
131 recognized: α , β , and γ diversity. α diversity refers to the local diversity of a community, habitat or field
132 plot. β diversity refers to the differences in diversity between habitats and γ diversity to the total
133 diversity of a region (Colwell, 2009). In this study we focus on α diversity. α diversity can be expressed
134 with many different metrics. In this study we focus on species richness (S) expressed as the total number
135 of species in a plot of a given size. Hence, from here on forward we only refer to tree species richness,
136 used to express the local tree species diversity.

137 **2.1 Field Datasets**

138 Field data were used to calculate the reference values of tree species richness. We used 15 datasets:
139 one from Australia, two from South-East Asia, six from Africa, three from South America and three from
140 Central America (Figure 1). All field datasets used in this study have been previously collected and
141 published and have coincident airborne lidar data available. Each field dataset is labeled with a three-
142 letter code and contained information on tree location, species and diameter at breast height (DBH). All
143 datasets were collected by different organizations and research teams resulting in different data
144 characteristics (Table 1, SI1). Four datasets consisted of one large plot of 25 ha (*rob*, Australia and *rab*,

145 Gabon) or 50 ha (*dan*, Malaysia and *bci*, Panama). The other eleven datasets consisted of multiple (3-21)
146 smaller plots with sizes ranging from 0.16 ha to 4.0 ha.



147
148 *Figure 1: Location of field sites across the three continents, colors of each study site are consistent*
149 *throughout the paper. Gridlines indicate 10° intervals in longitudinal and latitudinal directions. The size*
150 *of the place markers represents the size of the total sampled area relative to each other.*

151

152 *Table 1: Information on the original plot size, the amount of total area sampled in the field and the*
 153 *source of the data which is either a website where the data are published and/or a publication in which*
 154 *the data are described further.*

Country	Project code	No. native plots	Total area (ha)	Source / Additional Information
Oceania				
Australia	<i>rob</i>	1	25	(Bradford <i>et al.</i> , 2014)
South-East Asia				
Malaysia	<i>dan</i>	1	50	https://forestgeo.si.edu/sites/asia/danum-valley
Malaysia	<i>sep</i>	9	36	https://www.forestplots.net/en/ (Jucker <i>et al.</i> , 2018)
Africa				
DRC	<i>mal</i>	21	21	(Bastin <i>et al.</i> , 2015)
DRC	<i>yan</i>	9	9	(Kearsley <i>et al.</i> , 2013)
Gabon	<i>rab</i>	1	25	https://forestgeo.si.edu/sites/africa/rabi (Memiaghe <i>et al.</i> , 2016)
Gabon	<i>lop</i>	11	9.5	AfriTRON plots, https://www.forestplots.net/en/ (Labrière <i>et al.</i> , 2018)
Gabon	<i>mon</i>	12	12	(Fatoyinbo <i>et al.</i> , 2017)
Gabon	<i>mab</i>	10	10	(Bastin <i>et al.</i> , 2015; Labrière <i>et al.</i> , 2018)
South America				
Peru	<i>tam</i>	6	6	RAINFOR plots https://www.forestplots.net/en/ (Boyd <i>et al.</i> , 2013)
Brazil	<i>s11</i>	8	1.44	http://www.paisagenslidar.cnptia.embrapa.br/webgis/
Brazil	<i>s12</i>	21	3.36	http://www.paisagenslidar.cnptia.embrapa.br/webgis/
Central America				
Costa Rica	<i>lsv</i>	18	9	https://tropicalstudies.org/carbono-project/ (Clark & Clark, 2000)
Costa Rica	<i>cha</i>	3	2	http://neoselvas.wordpress.uconn.edu/costa-rica/
Panama	<i>bci</i>	1	50	https://forestgeo.si.edu/sites/neotropics/barro-colorado-island (Lobo & Dalling, 2013)

155

156 In this study, we assessed the structure-richness relationship at three spatial resolutions (1.0, 0.25,
 157 0.0625 ha) because of the non-linear relationship between the number of tree species (S) and sampled
 158 area. We selected squares of 1.0 ha (100 x 100 m) because they are often-used in ecology and it has
 159 been shown that the spatial mismatch of plot location and remote sensing products is minimized at this
 160 resolution (Réjou-Méchain *et al.*, 2014). We used squares of 0.25 ha (50 x 50 m) because these yielded
 161 the best results describing the structure-diversity relationship in Gabon (Marselis *et al.*, 2019), and
 162 squares of 0.0625 ha (25 x 25 m) because they correspond to a resolution close to the GEDI footprint

163 size. The datasets were used at one, two or three of the aforementioned resolutions depending on the
 164 original plot size and the availability of stem maps or subplots (Table 1, full table in SI1). For each of the
 165 field sites we calculated S for the entire dataset and for each plot at each plot size (Table 2). Only live
 166 trees with a DBH ≥ 10 cm were included, to ensure consistency among datasets, and we removed all
 167 plots of each resolution in which more than 20% of the trees were not identified to the genus level.

168 *Table 2: The total number of species identified at each study site and the average (\bar{x}) and standard*
 169 *deviation (s) of the species richness for each of the three plot sizes expressed as $\bar{x} \pm s$ (including only live*
 170 *trees with DBH ≥ 10 cm).*

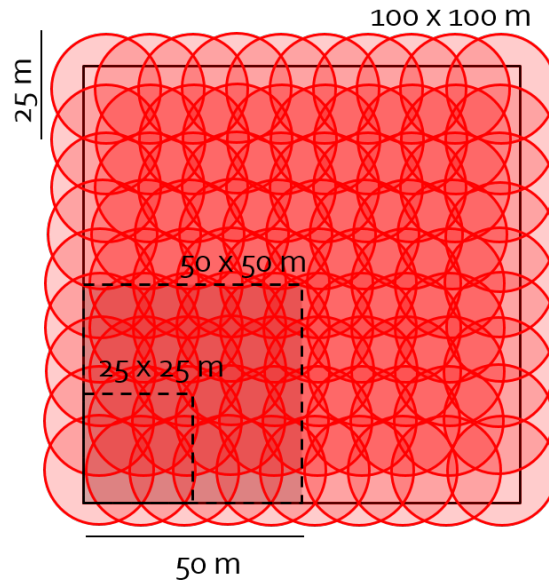
Country	Project Name	Total No. species	Total sampled area used (ha)	Species richness 1.0 ha	Species richness 0.25 ha	Species richness 0.0625 ha
<i>Oceania</i>						
Australia	<i>rob</i>	205	25	98 \pm 10	56 \pm 8	27 \pm 5
<i>South-East Asia</i>						
Malaysia	<i>dan</i>	260	6	117 \pm 13	51 \pm 7	19 \pm 4
Malaysia	<i>sep</i>	517	32	102 \pm 22	53 \pm 11	-
<i>Africa</i>						
DRC	<i>mal</i>	116	21	37 \pm 11	20 \pm 7	-
DRC	<i>yan</i>	232	9	50 \pm 23	24 \pm 13	10 \pm 6
Gabon	<i>rab</i>	234	25	84 \pm 8	42 \pm 6	17 \pm 4
Gabon	<i>lop</i>	118	9.5	32 \pm 22	17 \pm 10	8 \pm 4
Gabon	<i>mon</i>	146	12	32 \pm 15	15 \pm 9	7 \pm 5
Gabon	<i>mab</i>	196	10	55 \pm 8	-	-
<i>South America</i>						
Peru	<i>tam</i>	517	6	171 \pm 13	70 \pm 9	24 \pm 5
Brazil	<i>s11</i>	91	1.44	-	-	17 \pm 3
Brazil	<i>s12</i>	135	3.36	-	-	16 \pm 4
<i>Central America</i>						
Costa Rica	<i>lsv</i>	216	9	-	48 \pm 8	19 \pm 5
Costa Rica	<i>cha</i>	81	2	58	28 \pm 5	13 \pm 4
Panama	<i>bci</i>	220	50	87 \pm 8	42 \pm 6	17 \pm 3

171

172 2.2 Lidar Datasets

173 Each of the field datasets had coincident discrete return airborne laser scanning (ALS) data, or full-
 174 waveform lidar data from the Land Vegetation and Ice Sensor (LVIS), collected over the field plots within
 175 5 years of field data collection. We used the GEDI simulator (Hancock *et al.*, 2019) to create lidar

176 waveforms from the ALS data over the field plots. The ALS data was originally collected with a variety of
177 airborne instruments, but the GEDI simulator ensures a reliable GEDI-like waveform with minimal
178 influence of the original instrument-specific characteristics. In this way, all lidar information could be
179 processed in a consistent way across all study sites ensuring a reliable inter-comparison of canopy
180 structure metrics derived from the waveforms and allowing for easy transfer of the developed models to
181 future on-orbit GEDI data. Lidar waveforms were simulated with a 22 m ground footprint (Gaussian
182 distribution of laser energy, $\sigma = 5.5$ m). Lidar waveform locations were determined by filling each field
183 plot, using the original field plot size and shape, with footprint center locations 6.25 m from the plot
184 edge and 5 m between footprint center locations (Figure 2). In this way, a reliable measure of canopy
185 structure could be acquired for each plot by averaging lidar metrics from all waveforms inside the plot,
186 instead of using single waveforms in the plot center and evaluating structure-richness relationships
187 based on such potentially unrepresentative waveforms. The following information was extracted from
188 each simulated lidar waveform using mature and published algorithms: canopy height (expressed as the
189 98th percentile of the relative height metric; RH98), total Plant Area Index (PAI), and Plant Area Index at
190 a 1 m vertical resolution (Drake *et al.*, 2002; Tang *et al.*, 2012; Marselis *et al.*, 2018; Hancock *et al.*,
191 2019). The 1 m vertical profile was used to compare the canopy structure across the study sites. It was
192 aggregated into a 10 m vertical profile, summing all PAI values in each 10 m vertical bin, to be used in
193 the structure-richness analyses. We chose to use the PAI profile because it is a biophysical variable
194 describing the amount of plant material along the vertical forest axis, thus directly indicating the
195 occupation of vertical space. Marselis *et al.*, (2019) previously showed this information relates well to
196 tree species richness in Africa. The average of each of the resulting metrics from all waveforms within
197 each plot was computed to represent the canopy structure for each plot at each spatial resolution.



198
 199 *Figure 2: Illustration of simulated lidar waveform layout. The waveforms (red circles) have a Gaussian*
 200 *energy distribution with $\sigma=5.5$ m, resulting in a roughly 22 m diameter footprint. Example of simulated*
 201 *footprint distribution locations in a 1.0 (solid outline), 0.25 and 0.0625 ha field plot (dashed outline).*
 202 *Note: this footprint distribution was chosen to accurately depict canopy structure within the 0.0625, 0.25*
 203 *and 1.0 ha plots but it does not represent the spatial distribution of spaceborne GEDI waveforms.*

204 **2.3 Canopy Structure across the tropics**

205 To evaluate the canopy characteristics across the different study sites we calculated the median plant
 206 area volume density profile (composed of the PAI values for each 1 m vertical bin), using all simulated
 207 lidar waveforms for each study site. In addition to the median (50th percentile), we calculated the 10th,
 208 30th, 70th and 90th percentiles of the PAI values in the same 1 m vertical bins, to provide a representative
 209 distribution of the canopy structure across each study site.

210 **2.4 Species-area relationships across the tropics**

211 We created species-area relationships, calculating the mean and standard deviation of S for plot sizes
 212 ranging between 0.01 and 50 ha, to assess how species richness changes by plot size across our study
 213 sites. Each of the original field plots was filled with as many non-overlapping subplots as possible at 17
 214 spatial resolutions (0.01, 0.0225, 0.04, 0.09, 0.16, 0.25, 0.36, 0.64, 1.0, 2.25, 4.00, 6.25, 9.00, 12.25, 16.0,
 215 25.0, 50.0 ha) with each tree assigned to a subplot at each resolution. The plot sizes used at each study

216 site depended on the original plot size and the availability of stem maps (SI1). We visualized the mean
217 and standard deviation of S for each plot size at each study site to evaluate the differences in species-
218 area curves across the tropics.

219 **2.5 Structure-Richness Analysis**

220 To evaluate the existence of a relationship between vertical canopy structure and tree species richness
221 across the tropics, we developed models at three scales: local, regional and pan-tropical, because many
222 historical and environmental drivers of (tree) species diversity have stronger or weaker relations
223 depending on the scale of observation (Gaston, 2000; Keil & Chase, 2019) as do different ecosystem
224 functions (Chisholm *et al.*, 2013). Definitions of the scales are presented in the following sections.

225 **2.5.1 Local Analysis**

226 The local analysis focused on the structure-richness relationship within large (25 or 50 ha) plots. We
227 used data from adjacent field plots to evaluate the relationship between S and the canopy structure
228 expressed as canopy height (RH98), total PAI and vertical canopy profile (PAI at 10 m vertical intervals).

229 The local analysis was performed on data collected in *bci* (50 ha), *rab* and *rob* (25 ha). The other 50 ha
230 plot (*dan*) was not suitable for this analysis because the species identification was incomplete at the
231 time of analysis (Table 1). We related the canopy structure with S using a generalized linear model with
232 a Poisson error distribution. We used 5-fold cross-validation, extracting 20% of the data at random in
233 each fold as test data. We first performed feature selection on the training data, choosing the model
234 with the lowest Bayesian Information Criterion (BIC) score, and then constructed the predictive model
235 based on the same training data. We evaluated model performance using R^2 , Root Mean Squared
236 Difference as a percentage of the mean (RMSD%) and bias based on the predictions for the test data
237 (Piñeiro *et al.*, 2008). The average and 95% confidence interval of these metrics were recorded for each
238 study site at each resolution.

239 **2.5.2 Regional and Pan-tropical Analysis**

240 The regional analysis was focused on the structure-richness relationship based on non-adjacent plots
241 across study sites within the same biogeographical zone. We evaluated different combinations of study
242 sites at three spatial resolutions (Table 3). To prevent the large plots from dominating the regional and
243 pan-tropical analyses, we thinned their contribution to both the regional and pan-tropical datasets.
244 From the 25 ha plots we selected 1.0 ha plots at each corner, and from the 50 ha plots we selected all
245 corner and the middle plots along the long sides of the plot (6 1.0 ha plots total). To avoid mixing local
246 and regional effects, we employed a Monte-Carlo simulation approach in which we drew different
247 samples from the full regional dataset. In each Monte-Carlo run we randomly sampled one plot at the
248 given resolution from each original plot location (especially important at the 0.25 and 0.0625 ha
249 resolutions at which up to 16 plots exist at the location of each original 1.0 ha plot) and applied a cross-
250 validation (80/20) or leave-one-out cross validation (if $n \leq 25$) approach. In the cross-validation we again
251 performed a two-step approach: first we performed variable selection on the Poisson regression model
252 choosing the model with lowest BIC (using the *bestglm* package in R), and then built the predictive
253 model with the chosen variables. We applied the model to the test data and calculated the model
254 performance statistics for each fold according to Piñeiro *et al.* (2008).

255 The pan-tropical analysis focused on the structure-richness relationship combining the information from
256 all 15 study sites across all tropical regions, in other words, it was a special case of the regional analysis
257 in which data from all sites was included. Thus, the same methods were applied as in the regional
258 analysis.

259 *Table 3: Datasets used for regional and pan-tropical analysis of the structure-richness relationships. Note*
 260 *that one region may not contain the same number of plots across all resolutions due to limitations in the*
 261 *availability of subplot and stem map information, limiting the use of data from some study sites to only*
 262 *one or two resolutions.*

Region	Resolution (ha)	Study sites															Total
		<i>sep</i>	<i>dan</i>	<i>rob</i>	<i>lsv</i>	<i>cha</i>	<i>bci</i>	<i>tam</i>	<i>s11</i>	<i>s12</i>	<i>mal</i>	<i>yan</i>	<i>rab</i>	<i>mon</i>	<i>lop</i>	<i>mab</i>	
Africa	1										21	9	4	10	8	10	62
	0.25										21	9	4	11	11		56
	0.0625											9	4	12	11		36
South America	1																-
	0.25																-
	0.0625							6	8	21						35	
Central America	1																-
	0.25				18	3	6									27	
	0.0625				18	3	6									27	
South-East Asia	1	9	2													11	
	0.25	9	2													11	
	0.0625															-	
Pan-tropical	1	9	2	4		1	6	6			21	9	4	10	8	10	90
	0.25	9	2	4	18	3	6	6			21	9	4	11	11		104
	0.0625		6	4	18	3	6	6	8	21		9	4	12	11		108

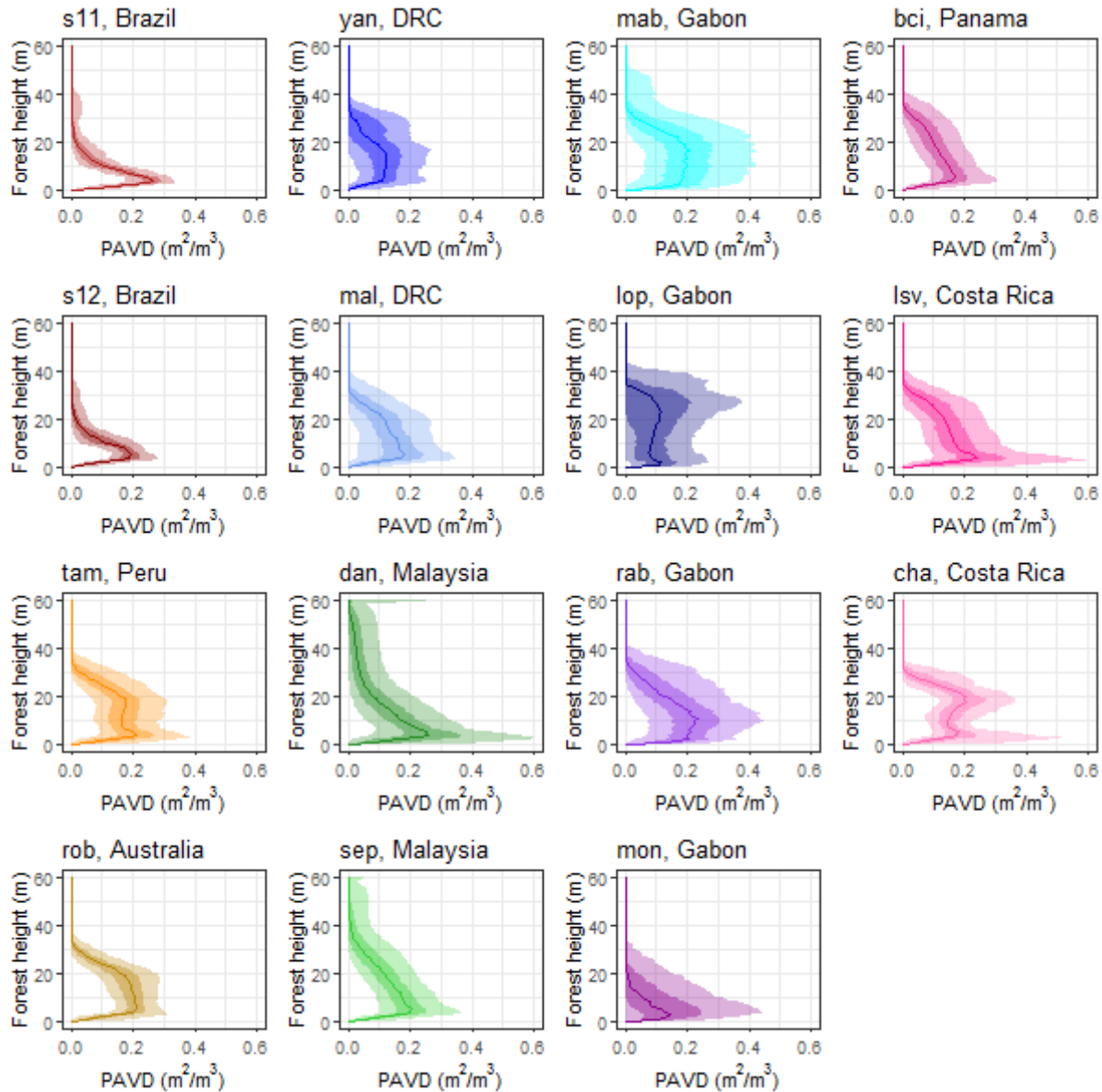
263

264 **3. Results**

265 **3.1 Vertical forest structure across lowland tropical moist forests**

266 The vertical canopy structure of forests, in terms of the vertical distribution of plant material varies
 267 between tropical regions (Figure 3). Maximum canopy height in our study sites in the Neotropics and
 268 Central Africa is typically around 40 m, and slightly lower in Australia, while canopy heights in South-East
 269 Asia exceed 60 m. Many sites show a distinct understory layer and a decrease in plant material through
 270 the canopy. Relative to the understory, the canopy layer sharply declines in vegetation density (*sep* and
 271 *dan*, Malaysia) or steadily declines along the vertical axis (*bci*, Panama; *rab*, Gabon; *mal*, DRC; *rob*,
 272 Australia). This vertical distribution of declining vegetation is exacerbated in degraded forests: in *s11*,
 273 *s12* (Brazil) and *mon* (Gabon), where the bulk of the vegetation exists close to the forest floor at ~5 m

274 height, but remnant trees in some plots may reach 40 m. Other sites, especially undisturbed ones, have
275 distinct canopy layers. In *tam* (Peru) and in the old-growth forest in *lsv* (Costa Rica) there are multiple
276 peaks of high-density vegetation across the vertical strata of the forest. The profiles of *yan* (DRC) and *lop*
277 (Gabon) are characterized by a multiple-peak pattern, with one peak 20-30 m in the canopy and another
278 within 5 m of the ground, reflecting the inherent structure of the forest-savanna mosaic. The less
279 disturbed *mab* (Gabon) forest shows high variability in canopy structure between plots (e.g. the wide
280 shaded area in Figure 3).



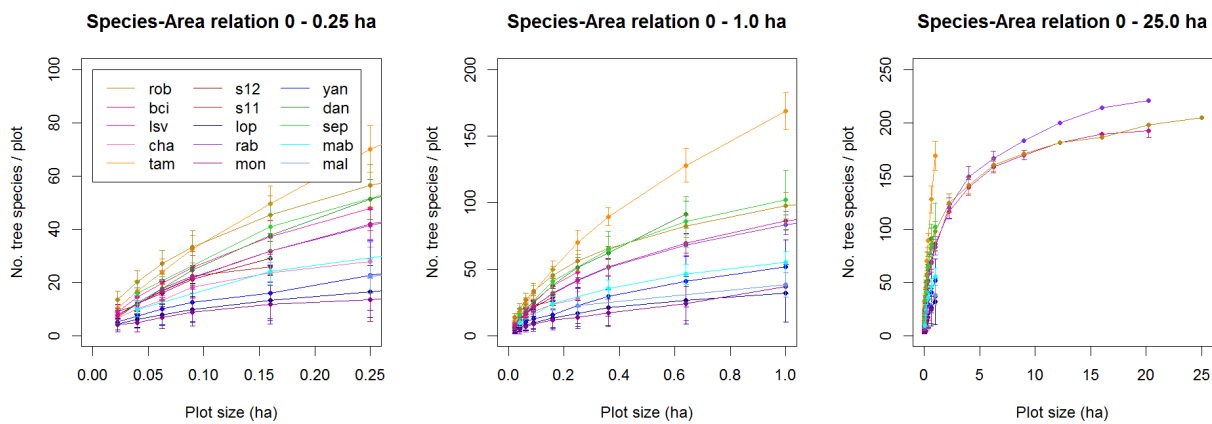
281
 282 *Figure 3: Canopy structure expressed as the Plant Area Volume Density profile (PAVD), expressing the*
 283 *Plant Area Index for each 1 m vertical bin, displayed as the median of all plots within each study site*
 284 *(solid line), the 30th-70th percentile (darker shaded area) and 10th-90th percentile (lighter shaded area).*

285

286 3.2 Species-area relationships

287 The number of species increases with plot size, but the rate of increase varies across study sites (Figure
 288 4). For example, in *rob* (Australia) 82-117 species occur in a 1.0 ha plot compared to 16-44 species in
 289 0.0625 ha plots. By contrast, *tam* (Peru) contains 154-185 species/ha, but only 11-35 species in a 0.0625

290 ha plot, similar to *rob*. Thus, species' composition of adjacent 0.0625 ha plots in *tam* must be more
 291 different from each other than adjacent 0.0625 ha plots in *rob* (Australia), in other words, the β diversity
 292 of the plots in *tam* is higher than in *rob*. The species-area curves vary in shape across study sites, with
 293 the highest total species richness in *tam* and lowest species richness in the African sites (Figure 4).
 294 Curves that are initially steep and decrease in slope at larger plot sizes indicate a high α diversity but a
 295 lower β diversity (e.g. when the area is increased, the same species are encountered).

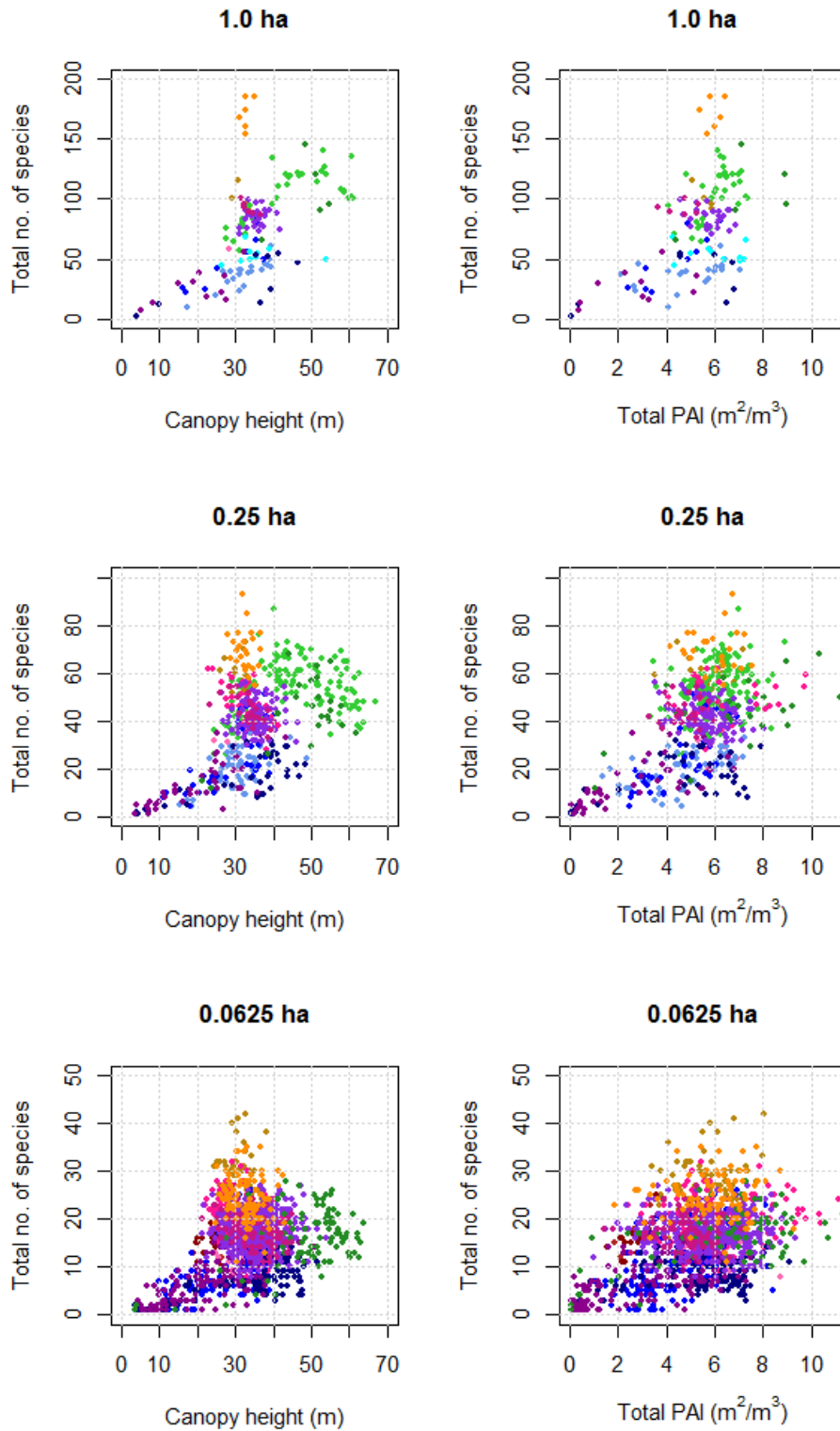


296
 297 *Figure 4: Relationships between tree species richness and area for each study site (note the change in y-*
 298 *axis across panels from left to right).*

299

300 3.3 Structure-richness relationships

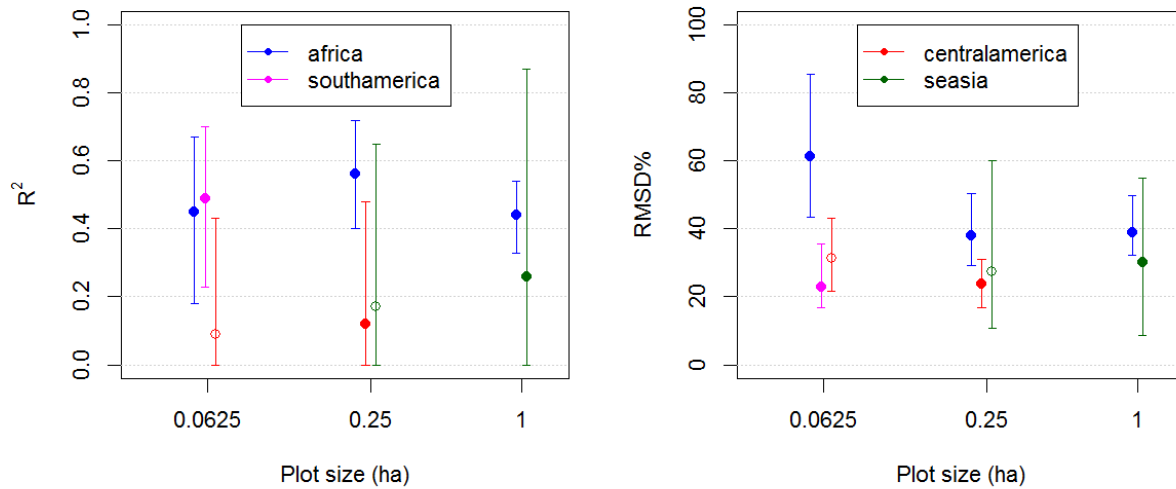
301 Pulling together the information on tree species richness and canopy structure (RH98 and Total PAI),
 302 species richness generally increases with increasing canopy height and increasing total Plant Area Index
 303 across the tropics (Figure 5).



304
 305 *Figure 5: Relation between canopy height (left) and total PAI (right) across three spatial scales for all*
 306 *study sites across the tropics. Each point represents one plot at the specific resolution. Dots are colored*
 307 *by study site corresponding according to legend in Figure 1.*

308 The cross-validation results of the local models reveal weak structure-richness relationships. Of the
309 three large plots (25 and 50 ha), only the models for *bci* (50 ha) show evidence of a significant
310 relationship between the predicted and observed values ($R^2=0.32$ at 1.0 ha, SI2). Even though species
311 richness within all three large plots can be predicted with a root mean squared error between 7-20% of
312 the mean species richness, the low RMSD% found only indicates that the predictions at the local scale
313 are close to the mean species richness, however in *rab* and *rob* the canopy structure is insensitive to the
314 local variation in tree species richness (see for example Figure SI2-1).

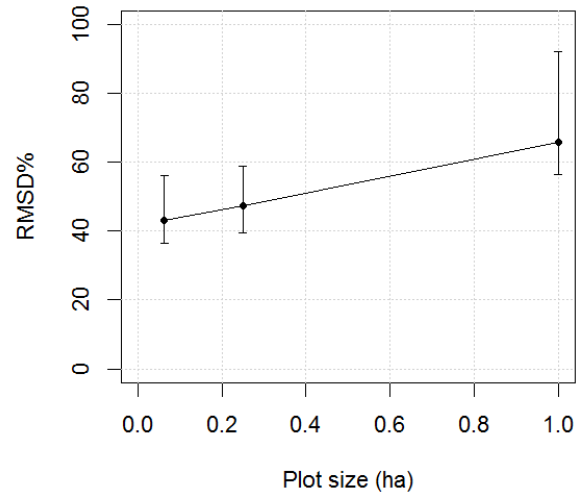
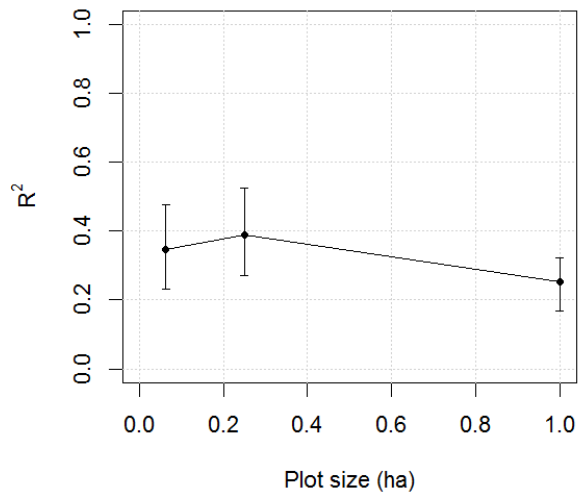
315 Regional structure-richness models generally show much better performance (Figure 6) than the local
316 models in terms of the variance in species richness that can be explained with the canopy structure
317 information (mostly significant models and higher R^2 values). However, prediction error (as percentage
318 of the mean species richness) is generally higher, partly due to the larger range in species richness in
319 these regional datasets. Regions of Africa and South America (Table 3) show the best model
320 performance whereas regions including the Costa Rica datasets show much poorer performance
321 (regions indicated with *centralamerica*). Results from an additional analysis on the compositional
322 similarity (Bray-Curtis; Faith *et al.*, 1987, SI3) of the Costa Rica dataset showed that, even though species
323 richness varies in Costa Rica (Table 2), the plots share many species, i.e. the composition is similar. In the
324 *africa* and *southamerica* datasets the variation in species richness is accompanied by a much larger
325 variation in species composition (SI3). The variation of the model performance for *seasia* is very high
326 because of the low number of plots available for this region and at the 0.25 ha resolution it was not
327 possible to create a significant model >95% of the monte-carlo iterations (Table 3). The model
328 performance does not provide clear results on the effect of the different resolutions, given the
329 overlapping error bars for models in the same region at multiple resolutions and the inability to create
330 each regional model at each spatial resolution (Figure 6).



331 *Figure 6: Cross-validated model performance of regional structure-richness models. Error bars indicate*
 332 *the 95% range of values for each performance metric. Solid dots indicate >95% of the generated models*
 333 *was statistically significant, open circles indicate a lower percentage was significant.*
 334

335 Pan-tropical structure-richness models show varying performance across the spatial resolutions with
 336 mean R^2 ranging between 0.25 and 0.39 and RMSD% between 66 and 43% for the plot sizes from 1.0
 337 and 0.0625 ha (Figure 7). However, the error bars of the model performance at different resolutions are
 338 overlapping, indicating that no resolution has a statistically better performance. Around 39% of the
 339 variation in tree species richness can be explained using canopy structure metrics alone at the 0.25 ha
 340 resolution at the pan-tropical scale. Sites with extremely high values of observed species richness are
 341 generally predicted poorly (SI4).

342



343

344 *Figure 7: Cross-validated model performance at the pan-tropical scale in terms of R^2 and RMSD%. Error*
 345 *bars indicate the range between which 95% of the performance values of the cross-validated models fall.*

346

347 **4. Discussion**

348 **4.1 Structure-richness relationships across scales**

349 In this study we explored the relationships between vertical canopy structure and tree species richness
350 at different resolutions across local, regional and pan-tropical scales, using a total of 15 study sites with
351 coincident lidar and field data across lowland tropical moist forests. We found weak relationships
352 between canopy structure and tree species richness at the local scale and the strongest relationship at
353 the regional scales in Africa and South America. We also found significant relationships between canopy
354 structure and tree species richness combining the data from all study sites.

355 At the local scale, within one large plot inside one forest type, the variation in the canopy structure is
356 determined largely by variability in growth structure within the same species (the 25 and 50 ha plots
357 have a similar composition throughout the plot, SI1 and SI3). For example, an adult tree of species X may
358 range in height from 20-40 m, so even though the canopy structure may differ between two plots of
359 similar composition, the difference is not attributed to a difference in species composition.

360 Furthermore, if a 20 m and 40 m tree of species X exist in the same plot, due to the difference in canopy
361 structure the model may predict a species richness of 2 based on variation in structure. On the other
362 hand, as area increases it is more likely that the difference in structure is caused by a difference in
363 composition. Individuals of most tropical forest species are spatially aggregated (Condit, 2000) so the
364 composition of two adjacent plots is more similar than the composition of two more distant plots. This is
365 the case for *bci*, where a 50 ha area with a species richness gradient was sampled (Fricker *et al.*, 2015)
366 and included in the local analysis, which led to more successful prediction of species richness based on
367 structure. Within the 25 ha plots sampled at *rab* and *rob*, the variation in composition is smaller and no
368 significant structure-richness relationships were found (SI3).

369 Increasing the scale, we found that regions consisting of sites exhibiting a large variation in species
370 composition among plots, but with a similar biogeographical history, show a much stronger structure-
371 richness relationship. However, we note that model performance differed quite drastically across
372 regions. The forest in *lsv*, Costa Rica, consists of largely similar species composition, whereas species
373 composition is much more different in regions where the structure-richness models perform better
374 (South-America, Africa), supporting the result from local scale models that species richness can be
375 better predicted from canopy structure in areas with greater β diversity.

376 At the pan-tropical scale we find a significant relationship between canopy structure and tree species
377 richness across all spatial resolutions. At the intermediate resolution (0.25 ha) this relationship appears
378 to be slightly stronger than at the higher and lower resolutions, but no significant difference was found.
379 However, the observed difference may be attributed to the lower sensitivity of species richness to rare
380 species at smaller plot sizes. For example, *tam* (Peru) plots have very high species richness at the 1.0 ha
381 resolution (Table 2), whereas at the 0.0625 ha resolution the species richness ranges between 11-35
382 species, which is still higher than most other sites but much less than at the 1.0 ha plot size. Because the
383 1.0 ha plot size captures more rare species in each plot, the 1.0 ha pan-tropical model predictions for
384 *tam* contain highly erroneous predictions that are not present in 0.0625 ha models (SI4). Rare species do
385 not contribute much to the canopy structure, thereby complicating the relationship between structure
386 and richness at a scale at which they contribute largely to species richness numbers.

387 **4.2 Limitations**

388 This research could be significantly improved by using more coincident lidar and field data to thoroughly
389 evaluate the existence and strength of the structure-richness relationship across all tropical regions.
390 However, the collection of such data is costly and time-consuming. Here, we were able to exploit 15
391 independently collected datasets (SI1). However, there are still large data gaps, especially in the Amazon

392 basin, the high biomass forests of Central Africa, the mainland of South-East Asia, New Guinea and
393 Australia, as well as the dry tropics and montane ecosystems. Apart from the spatial representation
394 problem, the low number of plots for certain regions attributes largely to the observed variability in
395 model performance. The pan-tropical models (with $n \geq 90$) show more stable performance than models
396 of regions with low numbers of plots (e.g. *seasia*). A training dataset that does not fully represent the
397 range of structure in the full dataset can lead to highly erroneous predictions for some of the test plots.
398 Such errors are exacerbated by the logarithmic link model in Poisson regression because errors can
399 increase exponentially. Even so, negative predictions are possible with linear regression and the risk of
400 underestimating tree species richness is higher for diverse areas. Hence, we chose to use Poisson
401 regression, knowing that it may lead to extreme predictions in some cases that should be accounted for
402 when operationalizing this method.

403 Species diversity can be identified in many different ways (Gotelli & Colwell, 2001; Colwell, 2009) and
404 there are risks and pitfalls using just one metric. In this study we only used 'species richness' (S), defined
405 by the number of different tree species in a defined area (the plot, with different sizes), as this metric is
406 easy to interpret and a prediction of the number of species/area can probably be used most directly by
407 ecosystem managers. Hereby we did not control for the number of stems in the plot, nor for the
408 abundance of the different species. Such things can be considered, for example, by using the Shannon
409 diversity index or rarefaction curves. Moreover, depending on the type of metric, a different model will
410 need to be selected. For example, a generalized linear regression with a Poisson error distribution, as
411 used here, is more suitable for estimated tree species richness as this is count data, whereas a linear
412 model with a Gaussian error distribution will be better suited for estimating Shannon diversity. Hence,
413 we chose to focus on one metric of diversity to test the structure-richness relationships, while
414 acknowledging other metrics may provide better, worse, or more useful predictions of tree species
415 diversity and these should be considered in the future.

416 This study serves as a first attempt to study the pan-tropical structure-richness relationship and should
417 be improved and further developed when more data become available. Additionally, the characteristics
418 of each dataset differed widely because all data were collected by different people and institutions. We
419 accounted for this as much as possible by using datasets only at reliable plot and subplot resolutions,
420 including only trees ≥ 10 cm DBH and including only plots with less than 20% of unidentified trees at the
421 genus level. Nonetheless, we acknowledge that the quality of the species identification varied and may
422 have affected our models as species identification in the tropics can be challenging due to the vast
423 variety of tree species and the fact that new species are still encountered. Species identification of new
424 and existing data could be improved using more botanists or genetic tests in the lab, which has been
425 done for some of the datasets used here, but is not yet feasible for all datasets. Additionally, including
426 information on species for trees with DBH ≥ 10 cm omits a lot of diversity found in the understory.
427 Fricker *et al.* (2015) showed that especially this diversity variation in small trees related well to the
428 canopy structure. Future research could determine if these findings are consistent across the tropics.

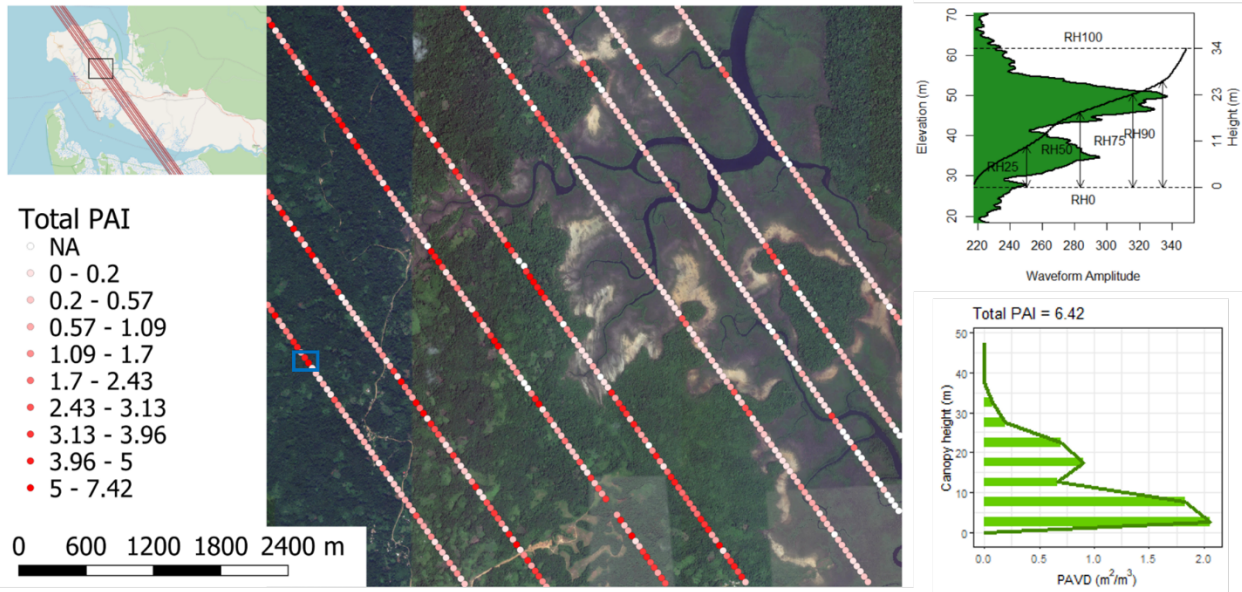
429 The availability of stem maps and subplots in each study site determined the spatial resolutions at which
430 datasets could be used. This resulted in the inclusion of different datasets for each region (Table 3). This
431 makes the comparison of model performance in the same region at different resolutions unreliable
432 because the models were not always built on the same data (plots and study sites), but we weighed this
433 decision to maximize the sizes of the datasets used to build the structure-richness models. Hence, no
434 conclusion can be drawn about the optimal resolution for the structure-richness relationships.

435 Accurate geolocation of field plots is key for the development of reliable species-richness models
436 (Fricker *et al.*, 2015). However, geolocation of field plots in the tropical forest can be challenging due to
437 difficulties receiving a reliable GPS signal under dense canopy. This should be taken into account,
438 especially when evaluating the performance of models build with small field plots, where the effects of
439 such geolocation errors will be larger (Réjou-Méchain *et al.*, 2014).

440 We included data from a range of forest stages, including old-growth forest, successional stages,
441 disturbed forest and even low tree density savanna sites. The relationships we found are partially driven
442 by this gradient (Figure 5). However, we deemed it essential to include data from across this range of
443 forest types, because if this method is to be operationalized using canopy structure information from
444 across the tropics, we will encounter all these different types of forest (Lewis *et al.*, 2015). We
445 acknowledge that many other variables could also be related to tree species richness across the tropics,
446 such as environmental variables as mean annual temperature and precipitation (Keil & Chase, 2019) or
447 topographical variables such as slope and elevation (Robinson *et al.*, 2018). However, in this study we
448 specifically focused on the relation between canopy structure and tree species diversity, in light of the
449 recently launched GEDI mission. We recognize that including such information on topographic and
450 environmental variables may further improve the mapping of tropical tree species richness.

451 **4.3 Future research & Applications**

452 Our results provide confidence regarding the existence of regional and pan-tropical structure-richness
453 relationships that may be used to map pan-tropical tree species richness. The most accurate predictions
454 seem to be achieved at the regional scale when adequate data are available and when forested areas
455 are grouped by regions of similar biogeographical history. However, in the absence of such data it may
456 be of more immediate interest to further develop pan-tropical models that were shown to explain up to
457 39% of variation in lowland moist forest tree species richness. At the time of writing, GEDI is collecting
458 canopy structure information close to the finest resolution tested here (0.0625 ha) and thus these data
459 may be well suited for mapping tropical tree species richness. GEDI is a sampling mission in which lidar
460 waveforms with 25 m diameter footprints are collected across 8 tracks with 600 m between-track
461 spacing, 60 m along-track spacing (Figure 8).



462
 463 *Figure 8: (a) Example of GEDI data captured over the east of Mondah forest, north-west of Libreville, in*
 464 *Gabon, Africa. The lidar waveforms are collected along-track with 8 tracks, a between-track spacing of*
 465 *600 m and an along-track spacing of 60 m. (b) shows an example GEDI waveform (shot number =*
 466 *31151117000411055, orbit = 03115, track = 05633) at the indicated location with the Relative Height*
 467 *metrics and (c) shows the accompanying PAI profile at 5 m vertical intervals from the Level-2 data*
 468 *product.*

469

470 The footprint-level GEDI information on vertical canopy structure is stored in the Level-2 data products

471 which are publicly available from the NASA Land Processes Distributed Active Archive Center (LPDAAC)¹.

472 GEDI gridded data products will have a 1 km² resolution in which the GEDI data samples are averaged to

473 1 km² values (Dubayah *et al.*, 2020). Our local scale models show that predictions of adjacent 0.0625 ha

474 plots (or in the future, footprints) are on average correct, but they will not detect local nuances in

475 species richness within forests of uniform composition. We suggest that the species richness predictions

476 could potentially be used in a similar way as for gridded GEDI data products and estimate the average

477 number of species/0.0625 ha within a 1 km² cell, as such information may still be of interest to local land

478 managers. Given the variable species-area relationships, it is not easy to translate species richness

479 predictions at 0.0625 ha resolution to the expected number of tree species in 1 km². Also, the amount of

¹ <https://lpdaac.usgs.gov/>

480 variance in species richness explained is limited. Therefore, we propose two future research avenues of
481 interest: fusion with spectral and/or radar data and using an environmental framework. Both spectral
482 data and radar data have previously been shown to predict some of the variance in tree species richness
483 (Foody & Cutler, 2006; Wolf *et al.*, 2012; Schäfer *et al.*, 2016; Bae *et al.*, 2019; Bongalov *et al.*, 2019;
484 Marselis *et al.*, 2019) and may improve our models and allow for more accurate predictions of tree
485 species richness across the tropics and the creation of wall-to-wall data products at higher spatial
486 resolution. Especially data from the hyperspectral HISUI (Matsunaga *et al.*, 2013) instrument, that is
487 soon to be launched to the International Space Station, the radar BIOMASS mission (Le Toan *et al.*,
488 2011), the ICESat-2 mission (Duncanson *et al.*, 2020) or the TanDEM-X mission (Qi *et al.*, 2019), may be
489 highly relevant for such applications. Alternatively, we believe that the inclusion of structural data within
490 previously developed environmental and biogeographical frameworks will help to predict tree species
491 diversity (Keil & Chase, 2019) as such frameworks already display intrinsic differences in tree species
492 diversity. Such frameworks could benefit from GEDI lidar data providing information on the occupation
493 of the vertical niche space and likely improve predictions of tropical tree species richness, which could
494 then be compared to existing predictions such as from Slik *et al.* (2015).

495 **5. Conclusions**

496 In this study we evaluated the existence of local, regional and pan-tropical relationships between
497 vertical canopy structure and tree species richness in the lowland moist forested tropics at three spatial
498 resolutions: 1.0, 0.25, and 0.0625 ha. Full-waveform lidar data provides detailed information on the
499 differences in vertical canopy structure between forests. Our results show that canopy structure can
500 explain a significant percentage of variation in tree species richness across different biogeographical
501 regions. A full set of regional structure-richness models will most likely aid accurate pan-tropical species
502 richness mapping, but the development of such a set of models is contingent on the availability of
503 sufficient coincident field & lidar data across the tropics. Using one single predictive model at a pan-
504 tropical scale, 39% of the variation in tree species richness could be explained using the vertical canopy
505 structure. Given this canopy structure can be derived directly from GEDI waveforms at the footprint
506 level, this provides an interesting avenue for mapping tree species richness at high spatial resolution.
507 Alternatively, canopy structure information from GEDI could be included in existing modeling
508 frameworks, combining structural with spectral, environmental and topographic information to create
509 more accurate tree species richness predictions.

510 References

- 511 Bae, S., Levick, S.R., Heidrich, L., Magdon, P., Leutner, B.F., Wollauer, S., Serebryanyk, A., Nauss, T.,
512 Krzystek, P., Gossner, M.M., Schall, P., Heibl, C., Bassler, C., Doerfler, I., Schulze, E., Krah, F.,
513 Culmsee, H., Jung, K., Heurich, M., Fischer, M., Seibold, S., Thorn, S., Gerlach, T., Hothorn, T.,
514 Weisser, W.W. & Muller, J. (2019) Radar vision in the mapping of forest biodiversity from space.
515 *Nature Communications*, **10**, 4757.
- 516 Bastin, J.F., Barbier, N., Réjou-Méchain, M., Fayolle, A., Gourlet-Fleury, S., Maniatis, D., De Haulleville, T.,
517 Baya, F., Beeckman, H., Beina, D., Couteron, P., Chuyong, G., Dauby, G., Doucet, J.L., Droissart, V.,
518 Dufrière, M., Ewango, C., Gillet, J.F., Gonmadje, C.H., Hart, T., Kavali, T., Kenfack, D., Libalah, M.,
519 Malhi, Y., Makana, J.R., Pélissier, R., Ploton, P., Serckx, A., Sonké, B., Stevart, T., Thomas, D.W., De
520 Cannière, C. & Bogaert, J. (2015) Seeing Central African forests through their largest trees. *Scientific*
521 *Reports*, **5**.
- 522 Bongalov, B., Burslem, D.F.R.P., Jucker, T., Thompson, S.E.D., Rosindell, J., Swinfield, T., Nilus, R.,
523 Clewley, D., Phillips, O.L. & Coomes, D.A. (2019) Reconciling the contribution of environmental and
524 stochastic structuring of tropical forest diversity through the lens of imaging spectroscopy. *Ecology*
525 *Letters*, **22**, 1608–1619.
- 526 Boyd, D.S., Hill, R.A., Hopkinson, C. & Baker, T.R. (2013) Landscape-scale forest disturbance regimes in
527 southern Peruvian Amazonia. *Ecological Applications*, **23**, 1588–1602.
- 528 Bradford, M.G., Metcalfe, D.J., Ford, A., Liddell, M.J. & McKeown, A. (2014) Floristics, stand structure
529 and aboveground biomass of a 25-ha rainforest plot in the wet tropics of Australia. *Journal of*
530 *Tropical Forest Science*, **26**, 543–553.
- 531 Carlson, K.M., Asner, G.P., Hughes, R.F., Ostertag, R. & Martin, R.E. (2007) Hyperspectral remote sensing
532 of canopy biodiversity in Hawaiian lowland rainforests. *Ecosystems*, **10**, 536–549.
- 533 Chisholm, R.A., Muller-Landau, H.C., Abdul Rahman, K., Bebbler, D.P., Bin, Y., Bohlman, S.A., Bourg, N.A.,
534 Brinks, J., Bunyavejchewin, S., Butt, N., Cao, H., Cao, M., Cárdenas, D., Chang, L.W., Chiang, J.M.,
535 Chuyong, G., Condit, R., Dattaraja, H.S., Davies, S., Duque, A., Fletcher, C., Gunatilleke, N.,
536 Gunatilleke, S., Hao, Z., Harrison, R.D., Howe, R., Hsieh, C.F., Hubbell, S.P., Itoh, A., Kenfack, D.,
537 Kiratiprayoon, S., Larson, A.J., Lian, J., Lin, D., Liu, H., Lutz, J.A., Ma, K., Malhi, Y., McMahan, S.,
538 Mcshea, W., Meegaskumbura, M., Mohd. Razman, S., Morecroft, M.D., Nytch, C.J., Oliveira, A.,
539 Parker, G.G., Pulla, S., Punchi-Manage, R., Romero-Saltos, H., Sang, W., Schurman, J., Su, S.H.,
540 Sukumar, R., Sun, I.F., Suresh, H.S., Tan, S., Thomas, D., Thomas, S., Thompson, J., Valencia, R.,
541 Wolf, A., Yap, S., Ye, W., Yuan, Z. & Zimmerman, J.K. (2013) Scale-dependent relationships between
542 tree species richness and ecosystem function in forests. *Journal of Ecology*, **101**, 1214–1224.
- 543 Clark, D.B. & Clark, D.A. (2000) Landscape-scale variation in forest structure and biomass in a tropical
544 rain forest. *Forest ecology and management*, **137**, 185–198.
- 545 Colwell, R.K. (2009) *Biodiversity: concepts, patterns and measurement. The Princeton guide to ecology*,
546 pp. 257–263.
- 547 Condit, R. (2000) Spatial patterns in the distribution of tropical tree species. *Science*, **288**, 1414–1418.
- 548 Corlett, R.T. & Primack, R.B. (2011) *Tropical Rain Forests: An Ecological and Biogeographical*
549 *Comparison: Second Edition*, 2nd edn. Blackwell Publishing.

550 Drake, J.B., Dubayah, R.O., Knox, R.G., Clark, D.B. & Blair, J.B. (2002) Sensitivity of large-footprint lidar to
551 canopy structure and biomass in a neotropical rainforest. *Remote Sensing of Environment*, **81**, 378–
552 392.

553 Dubayah, R.O., Blair, J.B., Goetz, S., Fatoyinbo, L., Hansen, M., Healey, S., Hofton, M., Hurtt, G., Kellner,
554 J., Luthcke, S., Armston, J., Tang, H., Duncanson, L., Hancock, S., Jantz, P., Marselis, S., Patterson, P.,
555 Qi, W. & Silva, C. (2020) The Global Ecosystem Dynamics Investigation: High-resolution laser
556 ranging of the Earth’s forests and topography. *Science of Remote Sensing*, **1**.

557 Duncanson, L., Neuenschwander, A., Hancock, S., Thomas, N., Fatoyinbo, T., Simard, M., Silva, C.A.,
558 Armston, J., Luthcke, S.B., Hofton, M., Kellner, J.R. & Dubayah, R. (2020) Biomass estimation from
559 simulated GEDI, ICESat-2 and NISAR across environmental gradients in Sonoma County, California.
560 *Remote Sensing of Environment*.

561 Faith, D.P., Minchin, P.R. & Belbin, L. (1987) Compositional dissimilarity as a robust measure of
562 ecological distance. *Vegetatio*, **69**, 57–68.

563 Fatoyinbo, T.E., Pinto, N., Simard, M., Armston, J., Duncanson, L., Hofton, M., Saatchi, S., Laval, M.,
564 Lou, Y., Denbina, M., Dubayah, R., Marselis, S.M., Tang, H., Hancock, S. & Hensley, S. (2017) The
565 2016 NASA AfriSAR campaign: airborne SAR and Lidar measurements of tropical forest structure
566 and biomass in support of future satellite missions. *IEEE Journal of Selected Topics in Applied Earth
567 Observations and Remote Sensing*, 4286–4287.

568 Féret, J.B. & Asner, G.P. (2014) Mapping tropical forest canopy diversity using high-fidelity imaging
569 spectroscopy. *Ecological Applications*, **24**, 1289–1296.

570 Foody, G.M. & Cutler, M.E.J. (2006) Mapping the species richness and composition of tropical forests
571 from remotely sensed data with neural networks. *Ecological Modelling*, **195**, 37–42.

572 Fricker, G.A., Wolf, J. a., Saatchi, S.S. & Gillespie, T.W. (2015) Predicting spatial variations of tree species
573 richness in tropical forests from high resolution remote sensing. *Ecological Applications*, **25**,
574 150218095111005.

575 Gaston, K.J. (2000) Global patterns in biodiversity. *Nature*, **405**, 220–227.

576 Gatti, R.C., Di Paola, A., Bombelli, A., Noce, S. & Valentini, R. (2017) Exploring the relationship between
577 canopy height and terrestrial plant diversity. *Plant Ecology*, **218**, 899–908.

578 Givnish, T.J. (1999) On the causes of gradients in tropical tree diversity. *Journal of Ecology*, **87**, 193–210.

579 Gotelli, N.J. & Colwell, R.K. (2001) Quantifying biodiversity: procedures and pitfalls in the measurement
580 and comparison of species richness. *Ecology Letters*, **4**, 379–391.

581 Hancock, S., Armston, J., Hofton, M., Sun, X., Tang, H., Duncanson, L.I., Kellner, J.R. & Dubayah, R. (2019)
582 The GEDI Simulator: A Large-Footprint Waveform Lidar Simulator for Calibration and Validation of
583 Spaceborne Missions. *Earth and Space Science*, **6**, 294–310.

584 Jucker, T., Asner, G.P., Dalponte, M., Brodrick, P.G., Philipson, C.D., Vaughn, N.R., Arn Teh, Y., Brelsford,
585 C., Burslem, D.F.R.P., Deere, N.J., Ewers, R.M., Kvasnica, J., Lewis, S.L., Malhi, Y., Milne, S., Nilus, R.,
586 Pfeifer, M., Phillips, O.L., Qie, L., Renneboog, N., Reynolds, G., Riutta, T., Struebig, M.J., Svátek, M.,
587 Turner, E.C. & Coomes, D.A. (2018) Estimating aboveground carbon density and its uncertainty in
588 Borneo’s structurally complex tropical forests using airborne laser scanning. *Biogeosciences*, **15**,
589 3811–3830.

- 590 Kearsley, E., De Haulleville, T., Hufkens, K., Kidimbu, A., Toirambe, B., Baert, G., Huygens, D., Kebede, Y.,
591 Defourny, P., Bogaert, J., Beeckman, H., Steppe, K., Boeckx, P. & Verbeeck, H. (2013) Conventional
592 tree height-diameter relationships significantly overestimate aboveground carbon stocks in the
593 Central Congo Basin. *Nature Communications*, **4**.
- 594 Keil, P. & Chase, J.M. (2019) Global patterns and drivers of tree diversity integrated across a continuum
595 of spatial grains. *Nature Ecology and Evolution*, **3**, 390.
- 596 Kier, G., Mutke, J., Dinerstein, E., Ricketts, T.H., Küper, W., Kreft, H. & Barthlott, W. (2005) Global
597 patterns of plant diversity and floristic knowledge. *Journal of Biogeography*, **32**, 1107–1116.
- 598 Labrière, N., Tao, S., Chave, J., Scipal, K., Le Toan, T., Abernethy, K., Alonso, A., Barbier, N., Bissiengou, P.,
599 Casal, T. & others (2018) In Situ Reference Datasets From the TropiSAR and AfriSAR Campaigns in
600 Support of Upcoming Spaceborne Biomass Missions. *IEEE Journal of Selected Topics in Applied
601 Earth Observations and Remote Sensing*, 1–11.
- 602 Lewis, S.L., Edwards, D.P. & Galbraith, D. (2015) Increasing human dominance of tropical forests.
603 *Science*, **349**.
- 604 Liang, J., Crowther, T.W., Picard, N., Wiser, S., Zhou, M., Alberti, G., Schulze, E.D., McGuire, A.D.,
605 Bozzato, F., Pretzsch, H., De-Miguel, S., Paquette, A., Hérault, B., Scherer-Lorenzen, M., Barrett,
606 C.B., Glick, H.B., Hengeveld, G.M., Nabuurs, G.J., Pfautsch, S., Viana, H., Vibrans, A.C., Ammer, C.,
607 Schall, P., Verbyla, D., Tchebakova, N., Fischer, M., Watson, J. V., Chen, H.Y.H., Lei, X., Schelhaas,
608 M.J., Lu, H., Gianelle, D., Parfenova, E.I., Salas, C., Lee, E., Lee, B., Kim, H.S., Bruelheide, H., Coomes,
609 D.A., Piotta, D., Sunderland, T., Schmid, B., Gourlet-Fleury, S., Sonké, B., Tavani, R., Zhu, J., Brandl,
610 S., Vayreda, J., Kitahara, F., Searle, E.B., Neldner, V.J., Ngugi, M.R., Baraloto, C., Frizzera, L., Bařazy,
611 R., Oleksyn, J., Zawila-Niedźwiecki, T., Bouriaud, O., Bussotti, F., Finér, L., Jaroszewicz, B., Jucker, T.,
612 Valladares, F., Jagodzinski, A.M., Peri, P.L., Gonmadje, C., Marthy, W., O’Brien, T., Martin, E.H.,
613 Marshall, A.R., Rovero, F., Bitariho, R., Niklaus, P.A., Alvarez-Loayza, P., Chamuya, N., Valencia, R.,
614 Mortier, F., Wortel, V., Engone-Obiang, N.L., Ferreira, L. V., Odeke, D.E., Vasquez, R.M., Lewis, S.L.
615 & Reich, P.B. (2016) Positive biodiversity-productivity relationship predominant in global forests.
616 *Science*.
- 617 Lobo, E. & Dalling, J.W. (2013) Effects of topography, soil type and forest age on the frequency and size
618 distribution of canopy gap disturbances in a tropical forest. *Biogeosciences*, **10**, 6769–6781.
- 619 MacArthur, R.H. & Wilson, E.O. (1967) *The theory of Island Biogeography*, Princeton University Press,
620 Princeton and Oxford.
- 621 Marselis, S.M., Tang, H., Armston, J., Abernethy, K., Alonso, A., Barbier, N., Bissiengou, P., Jeffery, K.,
622 Kenfack, D., Labrière, N. & others (2019) Exploring the relation between remotely sensed vertical
623 canopy structure and tree species diversity in Gabon. *Environmental Research Letters*, **14**.
- 624 Marselis, S.M., Tang, H., Armston, J.D., Calters, K., Labrière, N. & Dubayah, R. (2018) Distinguishing
625 vegetation types with airborne waveform lidar data in a tropical forest-savanna mosaic: A case
626 study in Lopé National Park, Gabon. *Remote Sensing of Environment*, **216**, 626–634.
- 627 Matsunaga, T., Iwasaki, A., Tsuchida, S., Tani, J., Kashimura, O., Nakamura, R., Yamamoto, H.,
628 Tachikawa, T. & Rokugawa, S. (2013) *Current status of Hyperspectral Imager Suite (HISUI).*
629 *International Geoscience and Remote Sensing Symposium (IGARSS)*.
- 630 Memiaghe, H.R., Lutz, J.A., Korte, L., Alonso, A. & Kenfack, D. (2016) Ecological Importance of Small-

- 631 Diameter Trees to the Structure, Diversity and Biomass of a Tropical Evergreen Forest at Rabi,
632 Gabon. *PLoS ONE*, **11**.
- 633 Moles, A.T., Warton, D.I., Warman, L., Swenson, N.G., Laffan, S.W., Zanne, A.E., Pitman, A., Hemmings,
634 F.A. & Leishman, M.R. (2009) Global patterns in plant height. *Journal of Ecology*, **97**, 923–932.
- 635 Mutke, J. & Barthlott, W. (2005) Patterns of vascular plant diversity at continental to global scales.
636 *Biologische skrifter*, **55**, 521–531.
- 637 Newnham, G.J., Armston, J.D., Calders, K., Disney, M.I., Lovell, J.L., Schaaf, C.B., Strahler, A.H. & Danson,
638 F.M. (2015) Terrestrial laser scanning for plot-scale forest measurement. *Current Forestry Reports*,
639 **1**, 239–251.
- 640 Palace, M.W., Sullivan, F.B., Ducey, M.J., Treuhaft, R.N., Herrick, C., Shimbo, J.Z. & Mota-E-Silva, J. (2015)
641 Estimating forest structure in a tropical forest using field measurements, a synthetic model and
642 discrete return lidar data. *Remote Sensing of Environment*, **161**, 1–11.
- 643 Pereira, H.M., Ferrier, S., Walters, M., Geller, G.N., Jongman, R.H.G., Scholes, R.J., Bruford, M.W.,
644 Brummitt, N., Butchart, S.H.M., Cardoso, A.C., Coops, N.C., Dulloo, E., Faith, D.P., Freyhof, J.,
645 Gregory, R.D., Heip, C., Höft, R., Hurtt, G., Jetz, W., Karp, D.S., McGeoch, M.A., Obura, D., Onoda,
646 Y., Pettorelli, N., Reyers, B., Sayre, R., Scharlemann, J.P.W., Stuart, S.N., Turak, E., Walpole, M. &
647 Wegmann, M. (2013) Essential biodiversity variables. *Science*, **339**, 277–278.
- 648 Pereira, H.M., Leadley, P.W., Proenca, V., Alkemade, R., Scharlemann, J.P.W., Fernandez-Manjarres, J.F.,
649 Araujo, M.B., Balvanera, P., Biggs, R., Cheung, W.W.L., Chini, L., Cooper, H.D., Gilman, E.L.,
650 Guenette, S., Hurtt, G.C., Huntington, H.P., Mace, G.M., Oberdorff, T., Revenga, C., Rodrigues, P.,
651 Scholes, R.J., Sumaila, U.R. & Walpole, M. (2010) Scenarios for Global Biodiversity in the 21st
652 Century. *Science*, **330**, 1496–1501.
- 653 Piñeiro, G., Perelman, S., Guerschman, J.P. & Paruelo, J.M. (2008) How to evaluate models: Observed vs.
654 predicted or predicted vs. observed? *Ecological Modelling*, **216**, 316–322.
- 655 Qi, W., Saarela, S., Armston, J., Stahl, G. & Dubayah, R. (2019) Forest biomass estimation over three
656 distinct forest types using TanDEM-X InSAR data and simulated GEDI lidar data. *Remote Sensing of*
657 *Environment*, **232**.
- 658 Réjou-Méchain, M., Muller-Landau, H.C., Detto, M., Thomas, S.C., Le Toan, T., Saatchi, S.S., Barreto-Silva,
659 J.S., Bourg, N.A., Bunyavejchewin, S., Butt, N., Brockelman, W.Y., Cao, M., Cárdenas, D., Chiang,
660 J.M., Chuyong, G.B., Clay, K., Condit, R., Dattaraja, H.S., Davies, S.J., Duque, A., Esufali, S., Ewango,
661 C., Fernando, R.H.S., Fletcher, C.D., N. Gunatilleke, I.A.U., Hao, Z., Harms, K.E., Hart, T.B., Hérault,
662 B., Howe, R.W., Hubbell, S.P., Johnson, D.J., Kenfack, D., Larson, A.J., Lin, L., Lin, Y., Lutz, J.A.,
663 Makana, J.R., Malhi, Y., Marthens, T.R., Mcewan, R.W., McMahon, S.M., Mcshea, W.J., Muscarella,
664 R., Nathalang, A., Noor, N.S.M., Nytch, C.J., Oliveira, A.A., Phillips, R.P., Pongpattananurak, N.,
665 Punchi-Manage, R., Salim, R., Schurman, J., Sukumar, R., Suresh, H.S., Suwanvecho, U., Thomas,
666 D.W., Thompson, J., Uriarte, M., Valencia, R., Vicentini, A., Wolf, A.T., Yap, S., Yuan, Z., Zartman,
667 C.E., Zimmerman, J.K. & Chave, J. (2014) Local spatial structure of forest biomass and its
668 consequences for remote sensing of carbon stocks. *Biogeosciences*, **11**, 6827–6840.
- 669 Robinson, C., Saatchi, S., Clark, D., Hurtado Astaiza, J., Hubel, A.F. & Gillespie, T.W. (2018) Topography
670 and Three-Dimensional Structure Can Estimate Tree Diversity along a Tropical Elevational Gradient
671 in Costa Rica. *Remote Sensing*, **10**, 629.

- 672 Rocchini, D., Boyd, D.S., Féret, J.B., Foody, G.M., He, K.S., Lausch, A., Nagendra, H., Wegmann, M. &
673 Pettorelli, N. (2016) Satellite remote sensing to monitor species diversity: potential and pitfalls.
674 *Remote Sensing in Ecology and Conservation*, **2**, 25–36.
- 675 Schäfer, E., Heiskanen, J., Heikinheimo, V. & Pellikka, P. (2016) Mapping tree species diversity of a
676 tropical montane forest by unsupervised clustering of airborne imaging spectroscopy data.
677 *Ecological Indicators*, **64**, 49–58.
- 678 Skidmore, A.K., Pettorelli, N., Coops, N.C., Geller, G.N., Hansen, M., Lucas, R., Mucher, C.A., O'Connor, B.,
679 Paganini, M., Pereira, H.M., Schaepman, M.E., Turner, W., Wang, T.J. & Wegmann, M. (2015) Agree
680 on biodiversity metrics to track from space. *Nature*, **523**, 403–405.
- 681 Slik, J.W.F., Arroyo-Rodríguez, V., Aiba, S.-I., Alvarez-Loayza, P., Alves, L.F., Ashton, P., Balvanera, P.,
682 Bastian, M.L., Bellingham, P.J., van den Berg, E., Bernacci, L., da Conceição Bispo, P., Blanc, L.,
683 Böhning-Gaese, K., Boeckx, P., Bongers, F., Boyle, B., Bradford, M., Brearley, F.Q., Breuer-
684 Ndoundou Hockemba, M., Bunyavejchewin, S., Calderado Leal Matos, D., Castillo-Santiago, M.,
685 Catharino, E.L.M., Chai, S.-L., Chen, Y., Colwell, R.K., Chazdon, R.L., Clark, C., Clark, D.B., Clark, D.A.,
686 Culmsee, H., Damas, K., Dattaraja, H.S., Dauby, G., Davidar, P., DeWalt, S.J., Doucet, J.-L., Duque, A.,
687 Durigan, G., Eichhorn, K.A.O., Eisenlohr, P. V., Eler, E., Ewango, C., Farwig, N., Feeley, K.J., Ferreira,
688 L., Field, R., de Oliveira Filho, A.T., Fletcher, C., Forshed, O., Franco, G., Fredriksson, G., Gillespie, T.,
689 Gillet, J.-F., Amarnath, G., Griffith, D.M., Grogan, J., Gunatilleke, N., Harris, D., Harrison, R., Hector,
690 A., Homeier, J., Imai, N., Itoh, A., Jansen, P.A., Joly, C.A., de Jong, B.H.J., Kartawinata, K., Kearsley,
691 E., Kelly, D.L., Kenfack, D., Kessler, M., Kitayama, K., Kooyman, R., Larney, E., Laumonier, Y.,
692 Laurance, S., Laurance, W.F., Lawes, M.J., Amaral, I.L. do, Letcher, S.G., Lindsell, J., Lu, X., Mansor,
693 A., Marjokorpi, A., Martin, E.H., Meilby, H., Melo, F.P.L., Metcalfe, D.J., Medjibe, V.P., Metzger, J.P.,
694 Millet, J., Mohandass, D., Montero, J.C., de Morisson Valeriano, M., Mugerwa, B., Nagamasu, H.,
695 Nilus, R., Ochoa-Gaona, S., Onrizal, Page, N., Parolin, P., Parren, M., Parthasarathy, N., Paudel, E.,
696 Permana, A., Piedade, M.T.F., Pitman, N.C.A., Poorter, L., Poulsen, A.D., Poulsen, J., Powers, J.,
697 Prasad, R.C., Puyravaud, J.-P., Razafimahaimodison, J.-C., Reitsma, J., dos Santos, J.R., Roberto
698 Spironello, W., Romero-Saltos, H., Rovero, F., Rozak, A.H., Ruokolainen, K., Rutishauser, E., Saiter,
699 F., Saner, P., Santos, B.A., Santos, F., Sarker, S.K., Satdichanh, M., Schmitt, C.B., Schöngart, J.,
700 Schulze, M., Suganuma, M.S., Sheil, D., da Silva Pinheiro, E., Sist, P., Stevart, T., Sukumar, R., Sun, I-
701 F., Sunderland, T., Suresh, H.S., Suzuki, E., Tabarelli, M., Tang, J., Targhetta, N., Theilade, I., Thomas,
702 D.W., Tchouto, P., Hurtado, J., Valencia, R., van Valkenburg, J.L.C.H., Van Do, T., Vasquez, R.,
703 Verbeeck, H., Adekunle, V., Vieira, S.A., Webb, C.O., Whitfeld, T., Wich, S.A., Williams, J., Wittmann,
704 F., Wöll, H., Yang, X., Adou Yao, C.Y., Yap, S.L., Yoneda, T., Zahawi, R.A., Zakaria, R., Zang, R., de
705 Assis, R.L., Garcia Luize, B. & Venticinque, E.M. (2015) An estimate of the number of tropical tree
706 species. *Proceedings of the National Academy of Sciences*, **112**, 7472–7477.
- 707 Slik, J.W.F., Franklin, J., Arroyo-Rodríguez, V., Field, R., Aguilar, S., Aguirre, N., Ahumada, J., Aiba, S.I.,
708 Alves, L.F., Anitha, K., Avella, A., Mora, F., Aymard, G.A.C., Báez, S., Balvanera, P., Bastian, M.L.,
709 Bastin, J.F., Bellingham, P.J., Van Den Berg, E., Da Conceição Bispo, P., Boeckx, P., Boehning-Gaese,
710 K., Bongers, F., Boyle, B., Brambach, F., Brearley, F.Q., Brown, S., Chai, S.L., Chazdon, R.L., Chen, S.,
711 Chhang, P., Chuyong, G., Ewango, C., Coronado, I.M., Cristóbal-Azkarate, J., Culmsee, H., Damas, K.,
712 Dattaraja, H.S., Davidar, P., DeWalt, S.J., Din, H., Drake, D.R., Duque, A., Durigan, G., Eichhorn, K.,
713 Eler, E.S., Enoki, T., Ensslin, A., Fandohan, A.B., Farwig, N., Feeley, K.J., Fischer, M., Forshed, O.,
714 Garcia, Q.S., Garkoti, S.C., Gillespie, T.W., Gillet, J.F., Gonmadje, C., Granzow-De La Cerda, I.,
715 Griffith, D.M., Grogan, J., Hakeem, K.R., Harris, D.J., Harrison, R.D., Hector, A., Hemp, A., Homeier,
716 J., Hussain, M.S., Ibarra-Manríquez, G., Hanum, I.F., Imai, N., Jansen, P.A., Joly, C.A., Joseph, S.,

717 Kartawinata, K., Kearsley, E., Kelly, D.L., Kessler, M., Killeen, T.J., Kooyman, R.M., Laumonier, Y.,
718 Laurance, S.G., Laurance, W.F., Lawes, M.J., Letcher, S.G., Lindsell, J., Lovett, J., Lozada, J., Lu, X.,
719 Lykke, A.M., Bin Mahmud, K., Mahayani, N.P.Di., Mansor, A., Marshall, A.R., Martin, E.H., Matos,
720 D.C.L., Meave, J.A., Melo, F.P.L., Mendoza, Z.H.A., Metali, F., Medjibe, V.P., Metzger, J.P., Metzker,
721 T., Mohandass, D., Munguía-Rosas, M.A., Muñoz, R., Nurtjahya, E., De Oliveira, E.L., Onrizal,
722 Parolin, P., Parren, M., Parthasarathy, N., Paudel, E., Perez, R., Pérez-García, E.A., Pommer, U.,
723 Poorter, L., Qi, L., Piedade, M.T.F., Pinto, J.R.R., Poulsen, A.D., Poulsen, J.R., Powers, J.S., Prasad,
724 R.C., Puyravaud, J.P., Rangel, O., Reitsma, J., Rocha, Di.S.B., Rolim, S., Rovero, F., Rozak, A.,
725 Ruokolainen, K., Rutishauser, E., Rutten, G., Mohd Said, M.N., Saiter, F.Z., Saner, P., Santos, B., Dos
726 Santos, J.R., Sarker, S.K., Schmitt, C.B., Schoengart, J., Schulze, M., Sheil, D., Sist, P., Souza, A.F.,
727 Spironello, W.R., Sposito, T., Steinmetz, R., Stevart, T., Suganuma, M.S., Sukri, R., Sultana, A.,
728 Sukumar, R., Sunderland, T., Supriyadi, Suresh, H.S., Suzuki, E., Tabarelli, M., Tang, J., Tanner, E.V.J.,
729 Targhetta, N., Theilade, I., Thomas, D., Timberlake, J., De Morisson Valeriano, M., Van Valkenburg,
730 J., Van Do, T., Van Sam, H., Vandermeer, J.H., Verbeeck, H., Vetaas, O.R., Adekunle, V., Vieira, S.A.,
731 Webb, C.O., Webb, E.L., Whitfeld, T., Wich, S., Williams, J., Wisner, S., Wittmann, F., Yang, X., Yao,
732 C.Y.A., Yap, S.L., Zahawi, R.A., Zakaria, R. & Zang, R. (2018) Phylogenetic classification of the world's
733 tropical forests. *Proceedings of the National Academy of Sciences of the United States of America*,
734 **115**, 1837–1842.

735 Ter Steege, H., Pitman, N.C.A., Killeen, T.J., Laurance, W.F., Peres, C.A., Guevara, J.E., Salomão, R.P.,
736 Castilho, C. V., Amaral, I.L., de Almeida Matos, F.D. & others (2015) Estimating the global
737 conservation status of more than 15,000 Amazonian tree species. *Science advances*, **1**, e1500936.

738 Sullivan, M.J.P., Talbot, J., Lewis, S.L., Phillips, O.L., Qie, L., Begne, S.K., Chave, J., Cuni-Sanchez, A.,
739 Hubau, W., Lopez-Gonzalez, G., Miles, L., Monteagudo-Mendoza, A., Sonké, B., Sunderland, T., Ter
740 Steege, H., White, L.J.T., Affum-Baffoe, K., Aiba, S.I., De Almeida, E.C., De Oliveira, E.A., Alvarez-
741 Loayza, P., Dávila, E.Á., Andrade, A., Aragão, L.E.O.C., Ashton, P., Aymard, G.A., Baker, T.R., Balinga,
742 M., Banin, L.F., Baraloto, C., Bastin, J.F., Berry, N., Bogaert, J., Bonal, D., Bongers, F., Brienen, R.,
743 Camargo, J.L.C., Cerón, C., Moscoso, V.C., Chezeaux, E., Clark, C.J., Pacheco, Á.C., Comiskey, J.A.,
744 Valverde, F.C., Coronado, E.N.H., Dargie, G., Davies, S.J., De Canniere, C., Djuikouo, M.N., Doucet,
745 J.L., Erwin, T.L., Espejo, J.S., Ewango, C.E.N., Fauset, S., Feldpausch, T.R., Herrera, R., Gilpin, M.,
746 Gloor, E., Hall, J.S., Harris, D.J., Hart, T.B., Kartawinata, K., Kho, L.K., Kitayama, K., Laurance, S.G.W.,
747 Laurance, W.F., Leal, M.E., Lovejoy, T., Lovett, J.C., Lukasu, F.M., Makana, J.R., Malhi, Y.,
748 Maracahipes, L., Marimon, B.S., Junior, B.H.M., Marshall, A.R., Morandi, P.S., Mukendi, J.T.,
749 Mukinzi, J., Nilus, R., Vargas, P.N., Camacho, N.C.P., Pardo, G., Peña-Claros, M., Pétronelli, P.,
750 Pickavance, G.C., Poulsen, A.D., Poulsen, J.R., Primack, R.B., Priyadi, H., Quesada, C.A., Reitsma, J.,
751 Réjou-Méchain, M., Restrepo, Z., Rutishauser, E., Salim, K.A., Salomão, R.P., Samsuedin, I., Sheil, D.,
752 Sierra, R., Silveira, M., Slik, J.W.F., Steel, L., Taedoumg, H., Tan, S., Terborgh, J.W., Thomas, S.C.,
753 Toledo, M., Umunay, P.M., Gamarra, L.V., Vieira, I.C.G., Vos, V.A., Wang, O., Willcock, S. &
754 Zemagho, L. (2017) Diversity and carbon storage across the tropical forest biome. *Scientific*
755 *Reports*, **7**, 39102.

756 Tang, H., Dubayah, R., Swatantran, A., Hofton, M., Sheldon, S., Clark, D.B. & Blair, B. (2012) Retrieval of
757 vertical LAI profiles over tropical rain forests using waveform lidar at La Selva, Costa Rica. *Remote*
758 *Sensing of Environment*, **124**, 242–250.

759 Le Toan, T., Quegan, S., Davidson, M.W.J., Balzter, H., Paillou, P., Papathanassiou, K., Plummer, S., Rocca,
760 F., Saatchi, S., Shugart, H. & Ulander, L. (2011) The BIOMASS mission: Mapping global forest
761 biomass to better understand the terrestrial carbon cycle. *Remote Sensing of Environment*.

- 762 Watson, J.E.M., Darling, E.S., Venter, O., Maron, M., Walston, J., Possingham, H.P., Dudley, N., Hockings,
763 M., Barnes, M. & Brooks, T.M. (2016) Bolder science needed now for protected areas. *Conservation*
764 *Biology*, **30**, 243–248.
- 765 Watson, J.E.M., Evans, T., Venter, O., Williams, B., Tulloch, A., Stewart, C., Thompson, I., Ray, J.C.,
766 Murray, K., Salazar, A., McAlpine, C., Potapov, P., Walston, J., Robinson, J.G., Painter, M., Wilkie, D.,
767 Filardi, C., Laurance, W.F., Houghton, R.A., Maxwell, S., Grantham, H., Samper, C., Wang, S.,
768 Laestadius, L., Runting, R.K., Silva-Chávez, G.A., Ervin, J. & Lindenmayer, D. (2018) The exceptional
769 value of intact forest ecosystems. *Nature Ecology and Evolution*, **2**, 599.
- 770 Wolf, J.A., Fricker, G.A., Meyer, V., Hubbell, S.P., Gillespie, T.W. & Saatchi, S.S. (2012) Plant species
771 richness is associated with canopy height and topography in a neotropical forest. *Remote Sensing*,
772 **4**, 4010–4021.
- 773

774 **Data Availability Statement**

775 Some of the field and lidar data used in this study can be downloaded directly from the internet. We
776 have grouped the data in three groups here: (i) LVIS lidar data, (ii) ALS lidar data and (iii) field data. All
777 datasets not mentioned in this statement were previously collected but have not been made publicly
778 available and were accessed through personal collaboration with the data providers.

779 **(i) LVIS lidar data**

780 The LVIS data for the *rab*, *lop*, *mon* and *mab* study sites can be downloaded from the NASA data archive
781 at the following DOI: <https://doi.org/10.3334/ORNLDAAC/1591>.

782 The LVIS data for the *cha* and *lsv* study sites is available on the following website:

783 <https://lvis.gsfc.nasa.gov/Data/Maps/CR2005Map.html>.

784 **(ii) ALS lidar data**

785 The ALS data over *rob* is available through the auscover data portal

786 ftp://qld.auscover.org.au/airborne_validation/lidar/robsons_creek/.

787 The ALS data over *s11* and *s12* can be downloaded from the sustainable landscapes data portal

788 <http://www.paisagenslidar.cnptia.embrapa.br/webgis/>.

789 **(iii) Field data**

790 Field data from *rob* has been published through the Terrestrial Ecosystem Research Network (TERN)

791 data portal linked from <https://supersites.tern.org.au/supersites/fnqr-robson>.

792 The *dan* and *rab* field data are all available through the Forestgeo website at

793 <https://forestgeo.si.edu/sites/asia/danum-valley>, <https://forestgeo.si.edu/sites/africa/rabi> and

794 <https://forestgeo.si.edu/sites/neotropics/barro-colorado-island>.

795 The *sep*, *lop* and *tam* field data are all available through forestplots.net and can be found under the
796 project names 'sepilok', 'lope' and 'tambopata' at <https://www.forestplots.net/en/>. These plots are part
797 of the T-FORCES, AfriTRON and RAINFOR continental plot networks.

798 The *mon* field data is archived through the NASA data archiving center and available at DOI:

799 <https://doi.org/10.3334/ORNLDAAAC/1580>.

800 The *s11* and *s12* were available through the data portals of the sustainable landscapes projects and can
801 be found under the field data from the São Félix do Xingu region collected in 2011 and 2012 in the
802 following data portal: <http://www.paisagenslidar.cnptia.embrapa.br/webgis/>.